Musculoskeletal Findings on Prostate MRI: Beyond Metastases

Justin Glavis-Bloom, MD; Roozbeh Houshyar, MD; Alexander Ushinsky, MD; Hanna Liu, MD; Thanh-Lan Bui, MA; Michelle Bardis, MS; Dylann K Fujimoto, BA; William A Grant, BS; Maryam Golshan-Momeni, MD; Joseph E Burns, MD, PhD

Prostate cancer causes more than 350,000 deaths worldwide each year and is one of the most commonly diagnosed male cancers.[1] Multiparametric prostate magnetic resonance imaging (mpMRI) is increasingly being employed for detection and classification of prostatic lesions to help reduce patient morbidity associated with invasive diagnosis and overtreatment of indolent lesions.[2] Modern prostate mpMRI is performed in accordance with the American College of Radiology Prostate Imaging Reporting and Data System (PI-RADS) imaging protocol. This protocol prescribes a limited field of view and specific set of sequences.[3] While this protocol affords standardization, there is often incomplete or limited evaluation of incidental findings beyond the prostate, many of which are musculoskeletal (MSK) lesions that can pose a diagnostic challenge to the interpreting radiologist. These may necessitate additional MRI sequences or imaging modalities to confirm diagnosis.

Affliations: Department of Radiology, University of California, Irvine Medical Center, Orange, CA (Drs Houshyar, Glavis-Bloom, Ushinsky, Liu, Golshan-Momeni, and Burns); UC Irvine School of Medicine, Irvine, CA (Ms Bui, Bardis, Fujimoto and Mr Grant).

Accurate interpretation of these findings on prostate MRI is critical to ensuring timely diagnosis, avoiding unnecessary testing, reducing costs, and minimizing patient anxiety. This review characterizes the MRI appearance of MSK lesions that may be encountered on prostate imaging. The lesions discussed here consist of the most clinically relevant findings likely to occur in patients undergoing prostate MRI, and are categorized by tissue of origin for simplicity.

Osseous and Chondral Lesions

Chordoma

Originating from embryonic notochord remnants, sacrococcygeal chordomas most frequently occur at the midline or paramedian sacrum and result in local bone destruction with associated soft tissue mass (Figure 1). These lesions typically contain gelatinous fluid, hemorrhages of different ages, and internal necrosis. Chordomas are characterized by low-to-intermediate T1 signal (sometimes with small foci of T1 hyperintensity), T2 hyperintensity, and moderate contrast enhancement. They occur most commonly in patients 60-80 years old.[4]

Chondrosarcoma

Pelvic chondrosarcomas commonly arise from the triradiate cartilage at the intersection of the ischium, ilium, and pubis. They typically demonstrate low-to-intermediate T1 signal, high T2 signal, and heterogeneous enhancement. Chondrosarcomas are most commonly located in the femur and iliac bones in patients 30-60 years old.[5]

Osteosarcoma

Osteosarcomas comprise multiple subtypes of malignant tumors characterized by osseous destruction, osteoid matrix formation, periosteal reaction, and soft tissue mass. Pelvic osteosarcomas in older patients are typically secondary to Paget disease or radiation. Findings include heterogeneous T1 signal intensity due to hemorrhage and calcification, high T2 signal of perilesional edema and soft tissue components, low T2 signal of calcified components, and enhancement of solid components.[5]

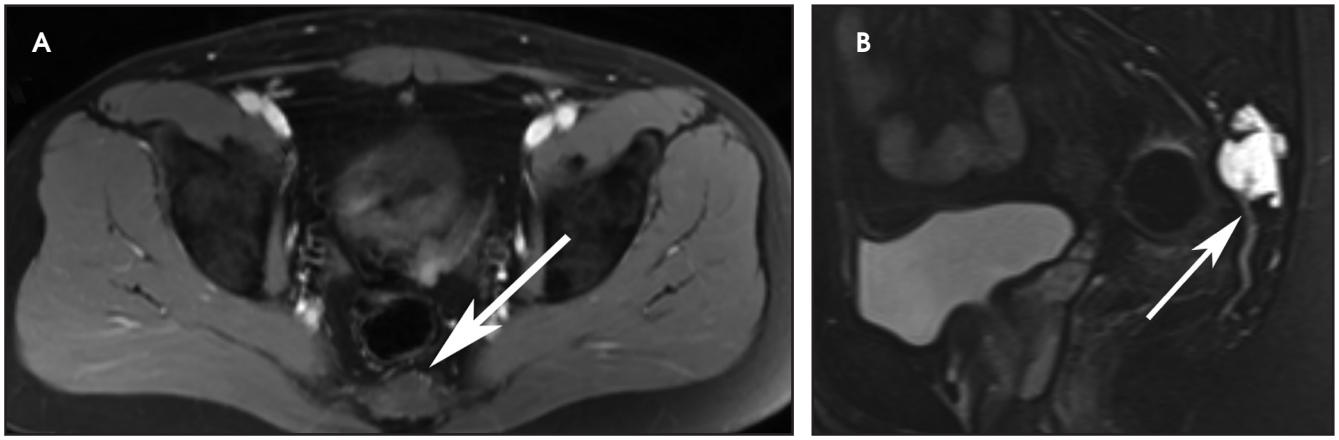

FIGURE 1. *Chordoma. Axial postcontrast fat-suppressed T1 image (A) demonstrates a mildly enhancing lesion in the sacrum enhancement (arrow). Sagittal fat-suppressed T2 image (B) demonstrates a T2 heterogeneously hyperintense sacral lesion compatible with a chordoma (arrow).*

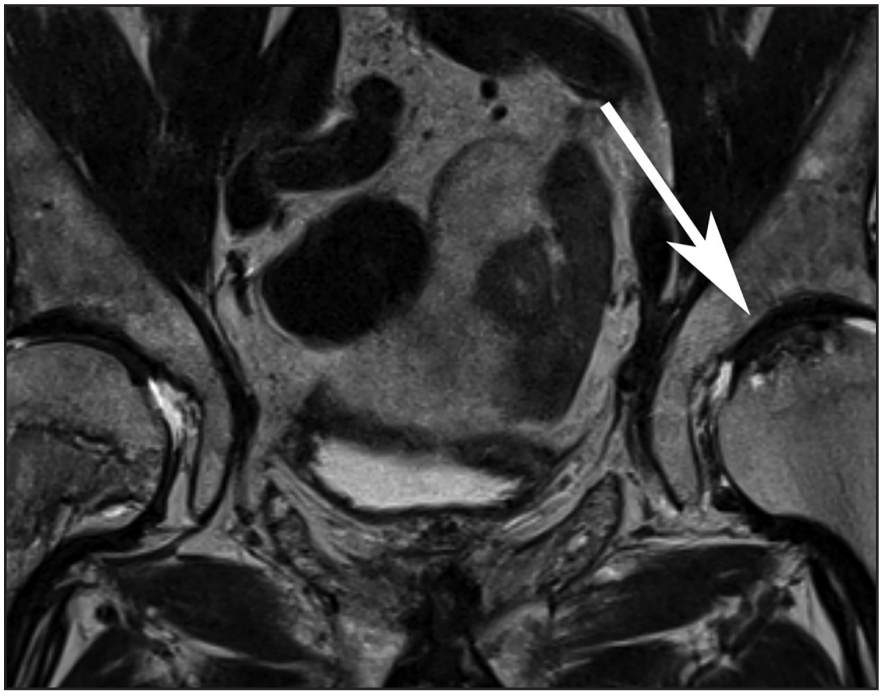

FIGURE 2. *Avascular necrosis. Coronal T2 image demonstrates irregular T2 hypointensity in the left femoral head with concentric surrounding edema, termed the "double line" sign (arrow).*

Avascular Necrosis

Avascular necrosis typically forms a central necrotic core surrounded by granulation tissue. T1 images demonstrate a single low-signal band (Figure 2). T2 images may demonstrate the pathognomonic "double line sign" between the hypointense outer normal/sclerotic tissues and hyperintense inner central ischemic/granulation tissue.[6]

Osteomyelitis

Osteomyelitis is characterized by confluent geographic regions of hypointense marrow signal on T1; hyperintense marrow signal on T2; and contrast enhancement due to increased blood flow from infection (Figure 3).[7]

Solitary Bone Cyst

Solitary (simple) bone cysts occur mostly in developing long bones and in the pelvis and spine of adults (Figure 4). These lesions demonstrate uniform high

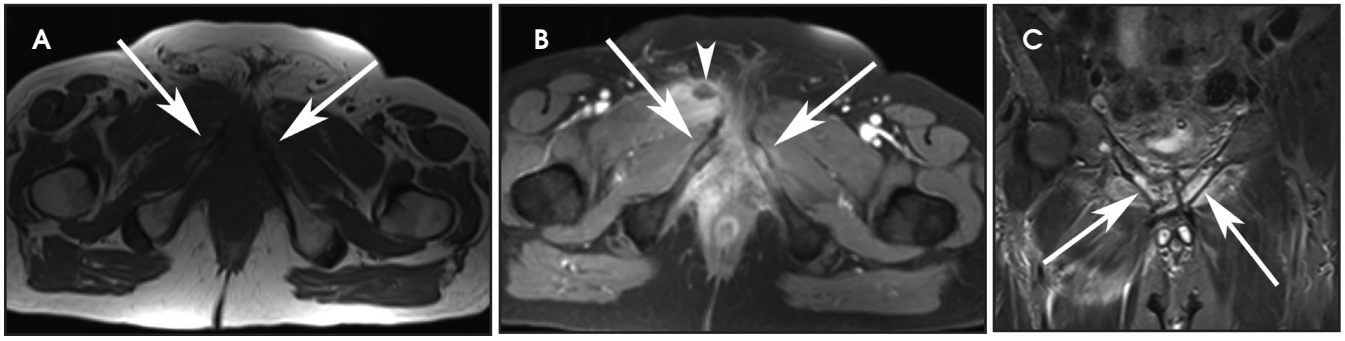

FIGURE 3. *Osteomyelitis. Axial T1 image (A) demonstrates confluent geometric areas of low T1 signal at the bilateral inferior pubic rami (arrows), with conjugate postcontrast axial fat-suppressed T1 (B) enhancement involving the adjacent soft tissues and adductor musculature with likely small abscess (arrowhead). Coronal fat-suppressed T2 image (C) demonstrates commensurate high signal consistent with marrow edema (arrows).*

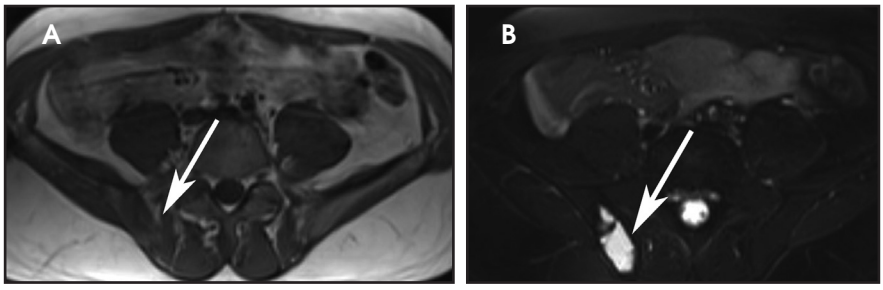

FIGURE 4. *Solitary bone cyst. Axial T1 image (A) demonstrates a T1 hypointense lesion in the right iliac bone (arrow). The lesion demonstrates increased T2 signal intensity on axial fat-suppressed T2 image (B), compatible with a bone cyst (arrow).*

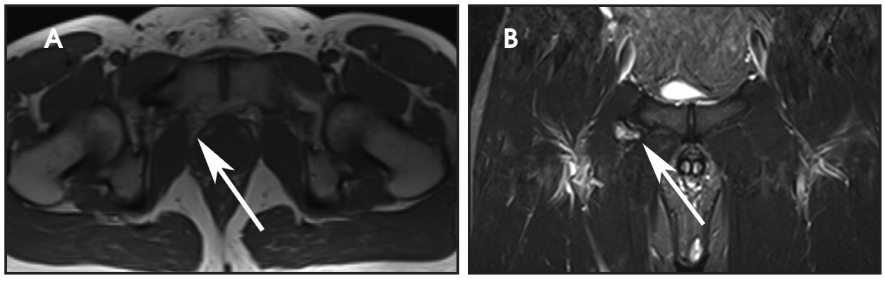

FIGURE 5. *Osteochondroma. Axial T1 image (A) demonstrates a T1 isointense to hypointense lesion in the right superior pubic ramus with cortical and medullary continuity to the underlying bone (arrow). There is increased T2 signal intensity on coronal fat-suppressed T2 image (B), compatible with cartilage cap (arrow).*

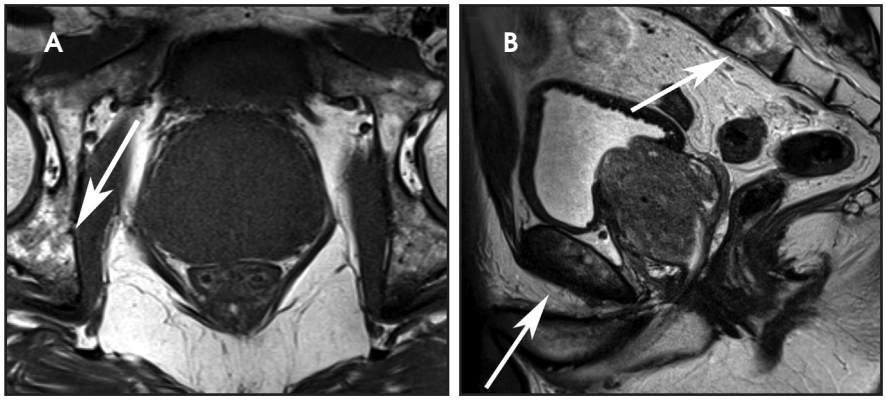

FIGURE 6. *Multiple myeloma. Axial T1 image (A) demonstrates diffusely heterogeneous hypointense bone-marrow signal throughout the visualized pelvis (arrow). Sagittal T2 image (B) demonstrates heterogeneous bone-marrow signal in the upper sacrum and pubic bone (arrows).*

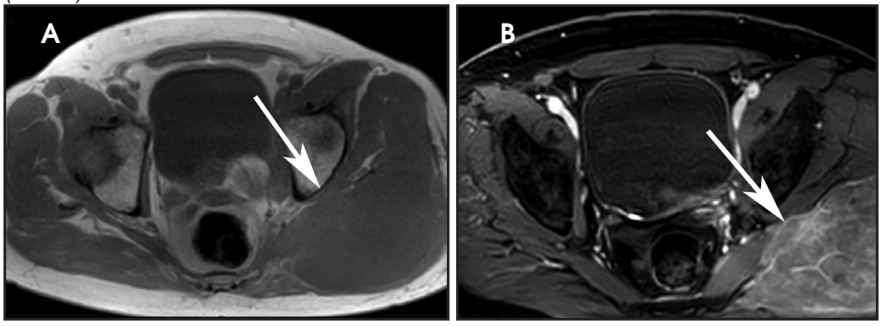

FIGURE 7. *Lymphoma. Axial T1 image (A) demonstrates an irregular T1 isointense mass at the left gluteus maximus and medius muscles. This demonstrates heterogeneous postcontrast fat-suppressed Axial T1 (B) enhancement (arrow). The mass extended through the left obturator foramen into the left perineum and through the left sciatic foramen (not shown).*

signal on T2 imaging corresponding to intralesional fluid and low T1 signal.[7] Postcontrast T1 imaging may be performed to verify the non-enhancing, cystic nature of the lesion.

Osteochondroma

Osteochondromas are overgrowths of bone often originating at the growth plate and are the most common benign bone tumors (Figure 5). They are continuous with the medullary space and covered by a cartilaginous cap, which demonstrates low T1 and high T2 signal. Mass effect and impingement are the most common associated complications. Malignant degeneration is rare, but may be suspected with enlargement of the cartilage cap beyond 1.5 cm.[7]

Paget Disease

Paget disease arises from accelerated bone remodeling, resulting in overgrowth and compromised structural integrity of affected bone. The skull, spine, pelvis, and long bones of the lower extremities are most often involved. Most patients are asymptomatic, with onset typically occurring after age 55. MRI features vary depending on disease stage: active disease is characterized by low T1 and high T2 signal corresponding to granulation tissue; longstanding disease demonstrates high T1 and T2 marrow signal corresponding to fat; and the late sclerotic phase is characterized by low T1 and T2 signal.[8]

Multiple Myeloma/Plasmacytoma

Multiple myeloma or solitary plasmacytoma originates in hematopoietic bone marrow and demonstrates marrow replacement, with decreased T1 signal and increased signal on T2 images with fat saturation (Figure 6). Plasmacytomas are generally larger than multiple myeloma lesions.[4]

Lymphoma

Lymphoma is characterized by permeative, moth-eaten osteolysis, reactive sclerosis, and soft tissue invasion (Figure 7). Secondary lymphoma arises from direct or hematogenous spread.

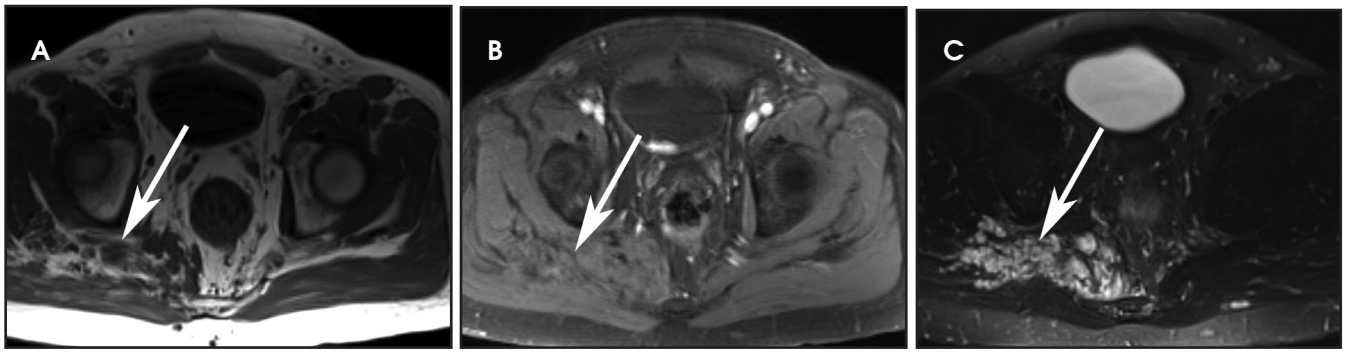

FIGURE 8. Benign/malignant peripheral nerve sheath tumors. Axial T1 image (A) demonstrates low T1 signal involving the right gluteus and piriformis muscles with subtle postcontrast fat-suppressed axial T1 (B) enhancement (arrows). Axial fat-suppressed T2 image (C) demonstrates hyperintensity with adjacent areas of low T2 signal from collagen islands (arrow).

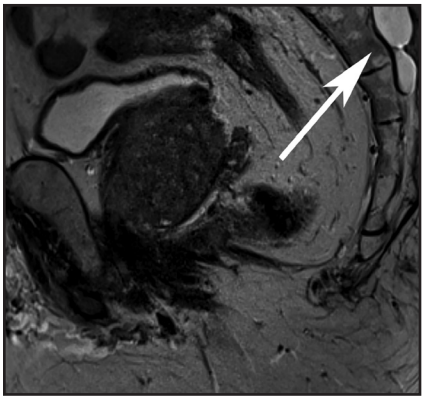

***FIGURE 9.** Perineural (Tarlov) cyst of the sacrum. Sagittal T2 image demonstrates T2 hyperintensity and characteristic location about the nerve roots at the sacral foramina (arrow).*

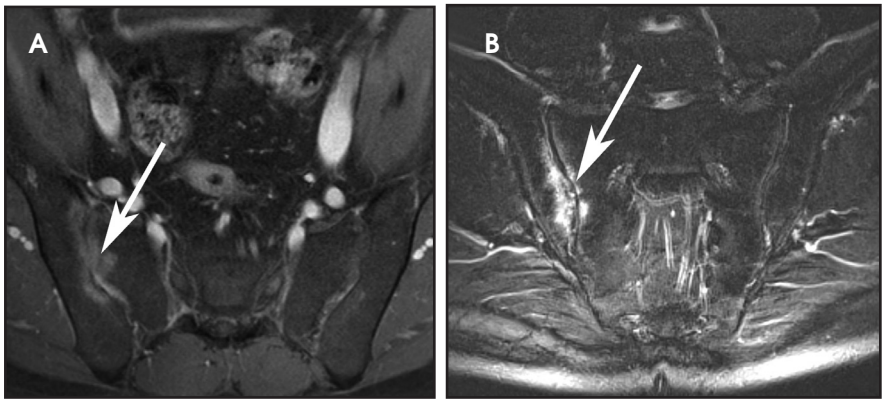

***FIGURE 10.** Sacroiliitis. Axial postcontrast fat-suppressed T1 image (A) demonstrates periarticular enhancement at the right sacroiliac joint (arrow). Fat-suppressed T2 image demonstrates increased signal at the joint on the axial (B) image (arrow), representing subchondral bone-marrow edema.*

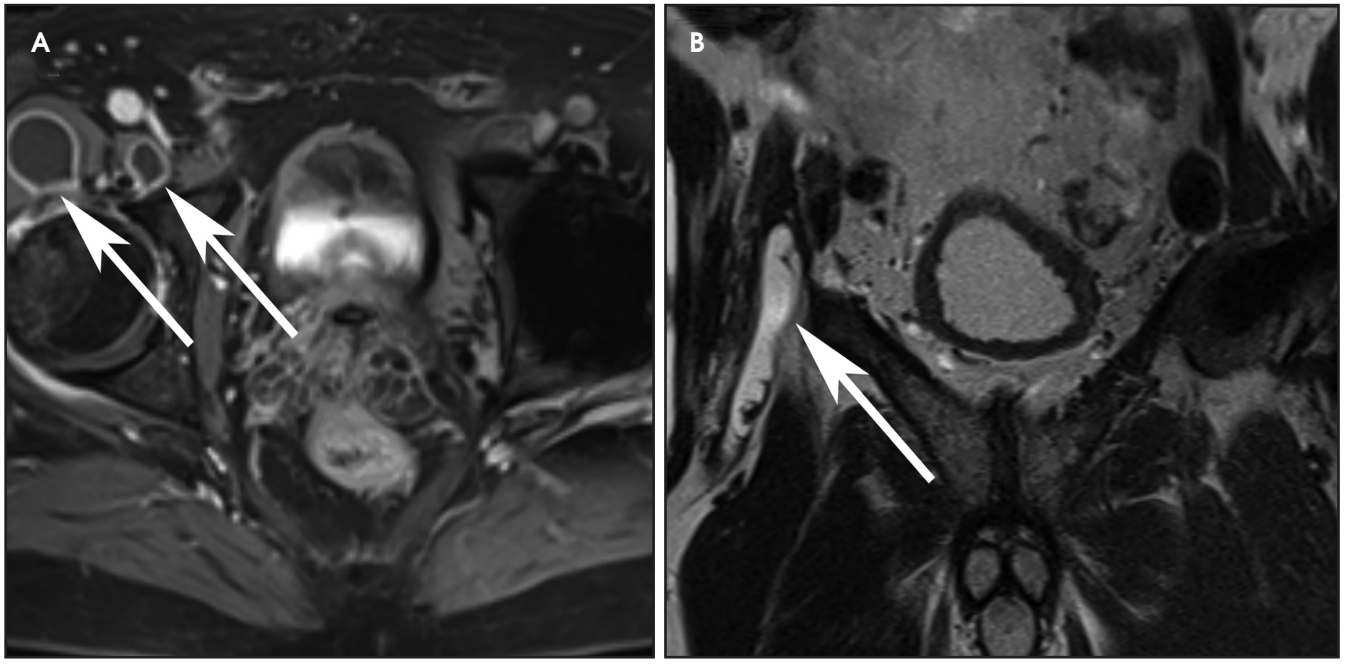

***FIGURE 11.** Iliopsoas bursitis. Axial postcontrast fat-suppressed T1 image (A) demonstrates a multi-loculated thin-walled cyst with thin peripheral postcontrast enhancement (arrows) compatible with an enlarged, inflamed iliopsoas bursa. T2 coronal image (B) demonstrates the enlarged bursa with high T2 signal corresponding to fluid (arrow).*

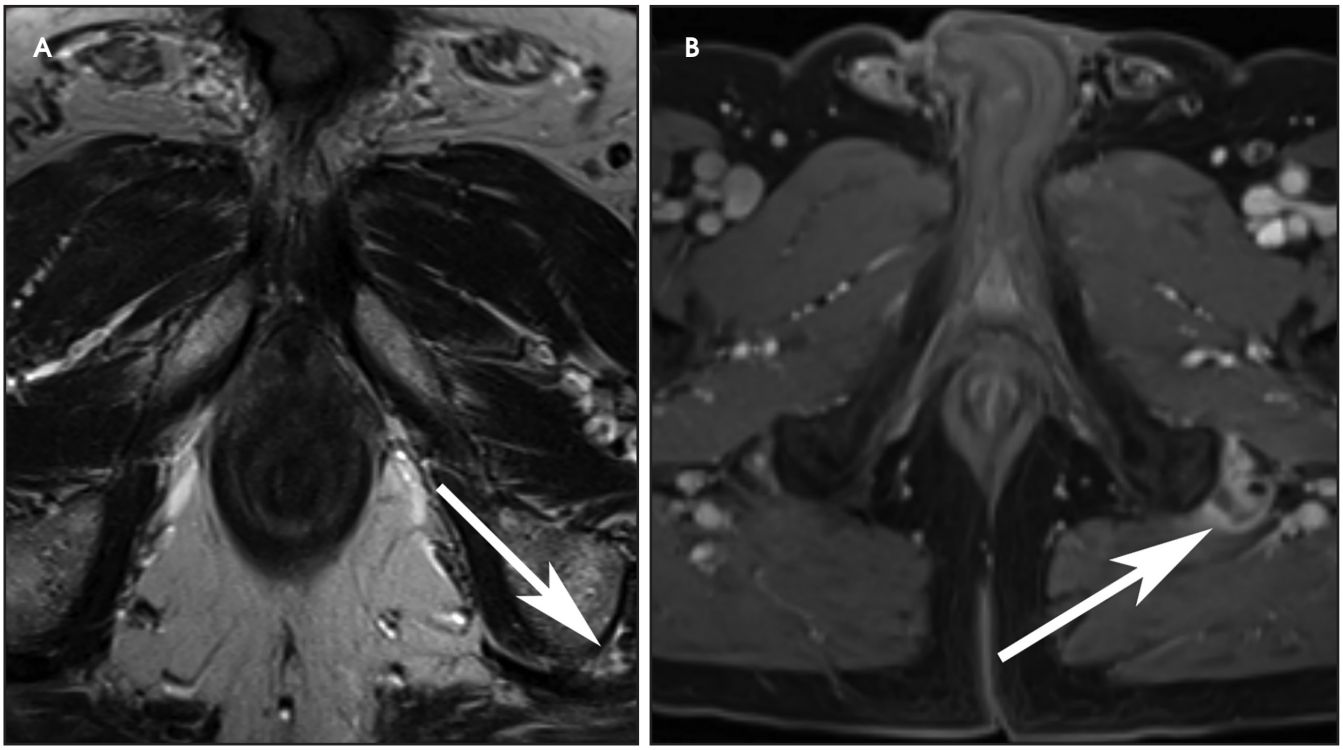

FIGURE 12. *Common hamstring origin tear/tendinopathy. Axial T2 image (A) demonstrate increased fluid signal adjacent to the left ischial tuberosity (arrow). The axial T1 postcontrast fat-suppressed image (B) demonstrates corresponding soft tissue enhancement (arrow). The findings are consistent with tendinopathy/partial tear of the left common hamstring origin.*

Substantial bone marrow invasion demonstrates areas of low T1 signal and high T2 signal. It occurs most often in the femur and pelvis for patients 30-85 years old.[9]

Perineural Lesions

Peripheral Nerve Sheath Tumors

Neurofibromas and schwannomas are common peripheral nerve sheath tumors comprising Schwann cells, fibroblasts, perineurial cells, and mast cells (Figure 8). Multiple neurofibromas are strongly associated with neurofibromatosis type 1, while multiple schwannomas are seen in neurofibromatosis type 2. These lesions demonstrate low T1 signal, homogeneous enhancement, and high T2 signal with adjacent areas of low T2 signal from collagen islands. Malignant peripheral nerve sheath tumors can arise de-novo or from malignant degeneration of benign tumors. Imaging characteristics suggestive of malignancy include rapid growth, irregular borders, and large lesion size.[4]

Perineural (Tarlov) Cysts of the Sacrum

Sacral perineural (Tarlov) cysts are meningeal dilatations in the spinal cord or sacral foramina with or without communication with the subarachnoid space (Figure 9). Perineural cysts are frequently asymptomatic and discovered incidentally; however, they can cause nerve root pain exacerbated by cough, or they may be associated with urinary, gastrointestinal, or neurological disorders. Perineural cysts are characterized by T2 hyperintensity.[4]

Articular and Periarticular Inflammation

Sacroiliitis

Sacroiliitis may be secondary to inflammatory or infectious processes. Patients often experience inflammatory pain in the lumbar region of the spine, hips, gluteal muscles, and lower extremities (Figure 10). Infectious sacroiliitis is of concern in cases of unilateral disease. Sacroiliitis is characterized by periarticular high T2 signal representing subchondral edema centered at the sacroiliac joint and postcontrast hyperenhancement.[10]

Synovitis

Synovitis is inflammation of the synovial membrane surrounding diarthrodial joint surfaces, bursae, and tendon sheaths. T2 hyperintensity and prominent postcontrast enhancement represents a thickened synovium with edema.[11]

Iliopsoas Bursitis

The iliopsoas bursa is located between the iliopsoas muscle and the anterior aspect of the hip joint (Figure 11). Bursitis may be multifactorial in etiology, including hip arthritis, overuse injury, septic arthritis, and trauma. Patients often present with groin pain that is exacerbated by hip flexion. Iliopsoas bursitis presents with an enlarged iliopsoas bursa, with high T2 signal and postcontrast enhancement of the bursal wall corresponding to inflammation.[12]

Muscular and Tendinous Processes

Common Hamstring Origin Tear/Tendinopathy

Common hamstring origin tear/tendinopathy occurs at the ischial tuberosity attachment of the hamstring muscles (Figure 12). This injury exhibits T2 hyperintensity at the myotendinous unit secondary to edema.[13]

Intramuscular Abscess

Intramuscular abscess is characterized by a precontrast low-to-intermediate T1-signal intensity and T2-hyperintensity, with an enhancing rim and central T1 hypointensity on postcontrast T1 fat saturation images. Adjacent muscle edema is characterized by T2 hyperintensity and muscle enlargement.[14]

Pleomorphic Undifferentiated Sarcoma

Previously known as fibrosarcoma or malignant fibrous histiocytoma, pleomorphic undifferentiated sarcomas (PUS) are the most common soft-tissue sarcomas. PUS is typically well circumscribed and located within or adjacent to muscle. Lesions demonstrate heterogeneous T1 signal due to hemorrhage, calcification, and necrosis; intermediate-to-high T2 signal; and avid contrast enhancement of the soft tissue component. PUS commonly occurs in patients 40-70 years old.[15]

Conclusion

Radiologists interpreting mpMRI of the prostate should be familiar with common, clinically significant incidental musculoskeletal lesions to ensure prompt and accurate diagnosis.

References

1. Bray F, Ferlay J, Soerjomataram I, et al. Global cancer statistics 2018: GLOBOCAN estimates of incidence and mortality worldwide for 36 cancers in 185 countries. *CA Cancer J Clin.* 2018; 68(6): 394-424.
2. Nguyentat M, Ushinsky A, Miranda-Aguirre A, et al. Validation of prostate imaging-reporting and data system version 2: A retrospective analysis. *Curr Probl Diagn Radiol.* 2018;47(6):404-409.
3. Weinreb JC, Barentsz JO, Choyke PL, et al. PI-RADS prostate imaging - reporting and data system: 2015, version 2. *Eur Urol.* 2016;69(1):16-40.
4. Gerber S, Ollivier L, Leclère J, et al. Imaging of sacral tumours. *Skeletal Radiol.* 2008;37(4):277-289.
5. Murphey MD, Andrews CL, Flemming DJ, et al. From the archives of the AFIP. Primary tumors of the spine: radiologic pathologic correlation. *Radiographics.* 1996;16(5):1131-1158.
6. Saini A, Saifuddin A. MRI of osteonecrosis. *Clin Radiol.* 2004;59(12):1079-1093.
7. Steffner R. Benign bone tumors. *Cancer Treat Res.* 2014;162:31-63.
8. Whitten CR, Saifuddin A. MRI of Paget's disease of bone. *Clin Radiol.* 2003;58(10):763-769.
9. Krishnan A, Shirkhoda A, Tehranzadeh J, et al. Primary bone lymphoma: radiographic-MR imaging correlation. *Radiographics.* 2003;23(6):1371-1383; discussion 1384-1387.
10. Rudwaleit M, Jurik AG, Hermann K-GA, et al. Defining active sacroiliitis on magnetic resonance imaging (MRI) for classification of axial spondyloarthritis: a consensual approach by the ASAS/OMERACT MRI group. *Ann Rheum Dis.* 2009;68(10):1520-1527.
11. Turan A, Celtikci P, Tufan A, et al. Basic radiological assessment of synovial diseases: a pictorial essay. *Eur J Rheumatol.* 2017;4(2):166-174.
12. Wunderbaldinger P, Bremer C, Schellenberger E, et al. Imaging features of iliopsoas bursitis. *Eur Radiol.* 2002;12(2):409-415.
13. Shelly MJ, Hodnett PA, MacMahon PJ, et al. MR imaging of muscle injury. *Magn Reson Imaging Clin N Am.* 2009;17(4):757-773
14. Garcia J. MRI in inflammatory myopathies. *Skeletal Radiol.* 2000;29(8):425-438.
15. Walker EA, Fenton ME, Salesky JS, et al. Magnetic resonance imaging of benign soft tissue neoplasms in adults. *Radiol Clin North Am.* 2011;49(6):1197-1217.